ISSN 1674-1056
http://cpb.iphy.ac.cn
http://iopscience.iop.org/cpb
中国物理 B
Chinese Physics
中国物理 Chinese Physics B

Research on influencing factors of performance in paintable carbon-based perovskite solar cells fabricated in ambient air

Wei-Kang Xu(许伟康), Feng-Xiang Chen(陈凤翔), Gong-Hui Cao(曹功辉), Jia-Qi Wang(王嘉绮), Li-Sheng Wang(汪礼胜)
Citation: Chin. Phys. B . 2018, 27(3): 038402. **doi:** 10.1088/1674-1056/27/3/038402

Journal homepage: http://cpb.iphy.ac.cn; http://iopscience.iop.org/cpb

What follows is a list of articles you may be interested in

Importance of ligands on TiO_2 nanocrystals for perovskite solar cells

Yao Zhao(赵耀), Yi-Cheng Zhao(赵怡程), Wen-Ke Zhou(周文可), Rui Fu(伏睿), Qi Li(李琪), Da-Peng Yu(俞大鹏), Qing Zhao(赵清)
Chin. Phys. B . 2018, 27(1): 018401. **doi:** 10.1088/1674-1056/27/1/018401

Improving power conversion efficiency of perovskite solar cells by cooperative LSPR of gold-silver dual nanoparticles

Peng Liu(刘鹏), Bing-chu Yang(杨兵初), Gang Liu(刘钢), Run-sheng Wu(吴闰生), Chu-jun Zhang(张楚俊), Fang Wan(万方), Shui-gen Li(李水根), Jun-liang Yang(阳军亮), Yong-li Gao(高永立), Cong-hua Zhou(周聪华)
Chin. Phys. B . 2017, 26(5): 058401. **doi:** 10.1088/1674-1056/26/5/058401

Dye-sensitized solar cell module realized photovoltaic and photothermal highly efficient conversion via three-dimensional printing technology

Qi-Zhang Huang(黄启章), Yan-Qing Zhu(朱艳青), Ji-Fu Shi(史继富), Lei-Lei Wang(王雷雷), Liu-Wen Zhong(钟柳文), Gang Xu(徐刚)
Chin. Phys. B . 2017, 26(3): 038401. **doi:** 10.1088/1674-1056/26/3/038401

Alleviating hysteresis and improving device stability of perovskite solar cells via alternate voltage sweeps

Chao Xia(夏超), Wei-Dong Song(宋伟东), Chong-Zhen Zhang(张崇臻), Song-Yang Yuan(袁松洋), Wen-Xiao Hu(胡文晓), Ping Qin(秦萍), Ru-Peng Wang(王汝鹏), Liang-Liang Zhao(赵亮亮), Xing-Fu Wang(王幸福), Miao He(何苗), Shu-Ti Li(李述体)
Chin. Phys. B . 2017, 26(1): 018401. **doi:** 10.1088/1674-1056/26/1/018401

Non-ionizing energy loss calculations for modeling electron-induced degradation of Cu(In, Ga)Se_2 thin-film solar cells

Ming Lu(鲁明), Jing Xu(徐晶), Jian-Wei Huang(黄建微)
Chin. Phys. B . 2016, 25(9): 098402. **doi:** 10.1088/1674-1056/25/9/098402

Factors influencing the performance of paintable carbon-based perovskite solar cells fabricated in ambient air*

Wei-Kang Xu(许伟康), Feng-Xiang Chen(陈凤翔)†, Gong-Hui Cao(曹功辉), Jia-Qi Wang(王嘉绮), and Li-Sheng Wang(汪礼胜)

Department of Physics Science and Technology, School of Science, Wuhan University of Technology, Wuhan 430070, *China*

(Received 17 October 2017; revised manuscript received 18 November 2017; published online 11 February 2018)

To date, many efforts have been made to improve the performance of paintable carbon-based (PC-based) perovskite solar cells (PSCs). Though great progress has been achieved, their power conversion efficiencies are still relatively low compared with hole-transport-materials-based PSCs. General research on influencing factors of performance in PC-based PSCs is still insufficient. In this work, PC-based PSCs were fabricated in ambient air and four groups of controlled experiments were performed in which the PbI_2 layers were prepared with or without antisolvent extraction treatment. These four groups of experiments were designed to find out the effect of different influencing factors on PC-based PSCs performance, for example, PbI_2 residual, the surface morphology of the perovskite film, the surface roughness of the perovskite film, and the contact status of the perovskite/carbon electrode interface. With a systematic analysis, we demonstrated that the contact status of the perovskite/carbon electrode interface played a vital role in PC-based PSCs, and a flat, smooth perovskite surface could help to improve this contact status significantly. Besides, on the precondition of a poor contact interface, no PbI_2 residual and a good surface morphology only brought limited benefits to the performances of PC-based PSCs.

Keywords: influencing factors, paintable carbon-based perovskite solar cells, contact status

PACS: 84.60.Jt, 88.40.H–, 84.60.Bk **DOI:** 10.1088/1674-1056/27/3/038402

1. Introduction

Since the organometal halide perovskite solar cells (PSCs) were first invented in 2009,[1] their power conversion efficiencies (PCEs) have been increased rapidly,[2–4] and they exhibited promising application prospects. Various methods have been developed to improve the photovoltaic performance of PSCs, such as two-step sequential deposition method,[5] vacuum flash-assisted method,[6] and solvent engineering method.[7] Such progress has partially removed obstacles for PSCs on the commercial road. However, most PSCs with high PCEs are usually hole-transport-materials-based (HTM-based), for which expensive hole transport materials (such as spiro-OMeTAD) and noble metal electrodes are usually indispensable.[8–11] Moreover, most fabrication techniques by now request a nitrogen protected atmosphere or a high vacuum environment, which increases the fabrication cost a lot and hinders the further industrialization.[12–14] In contrast, paintable carbon-based (PC-based) PSCs are comparatively low-cost both in material and the required equipment. They are hole-transport-layer-free and work efficiently because the perovskite material can simultaneously transport both electrons and holes.[15,16]

The carbon electrode is very cheap, stable, environment-friendly, and can be easily prepared by directly painting carbon paste on the perovskite layer with a low-temperature annealing process.[17] Though the PCEs of PC-based PSCs remain relatively low compared with those of HTM-based PSCs, their intrinsic advantages continue to inspire efforts to improve their performance. Wei and co-workers developed a new type of carbon film with good flexibility and conductivity that could be simply hot pressed onto the perovskite layer. A PCE up to 13.5% has been achieved.[18] Chen and co-workers utilized a solvent strategy based on the two-step sequential method to prepare the perovskite layer. A shiny and smooth perovskite surface was obtained and an outstanding PCE of 14.4% has been achieved.[19] It is widely recognized that the leading factor that influences the performance of HTM-based PSCs is the quality of the perovskite film, with aspects such as grain sizes, crystal boundaries, and surface coverage.[20] However, the working principle of PC-based PSCs is significantly different from that of HTM-based PSCs,[21] and the investigation on influencing factors of PC-based PSCs performance is still insufficient.

The antisolvent treatment method is usually directly applied to the perovskite layer[22] or on the PbI_2 layer in HTM-based PSCs.[20,23–25] Few pieces of literature about antisolvent treatments on PbI_2 layers in PC-based PSCs have been reported. In this work, we used three types of antisolvents (chlorobenzene (CB), toluene (TL), and diethyl ether (DE)) in the antisolvent extraction treatments on PbI_2 layers in PC-based PSCs to control the device qualities. At the same time, PSCs without (W/O) antisolvent treatment were also prepared as a reference. Comprehensive research on the influencing factors including PbI_2 residual, the surface morphology of the

*Project supported by the National Natural Science Foundation of China (Grant No. 51702245) and the Fundamental Research Funds for the Central Universities, China (Grant No. WUT: 2017IB013).

†Corresponding author. E-mail: phonixchen79@whut.edu.cn

© 2018 Chinese Physical Society and IOP Publishing Ltd

perovskite film, the surface roughness of the perovskite film, and the contact status of the perovskite/carbon electrode interface in PC-based PSCs was performed. Remarkably, all the preparation procedures were completed in the ambient air with a relative humidity about 40%. Humidity is one of the causes of variations in device performance.[26,27] We found that the primary factor is the contact status of the perovskite/carbon electrode interface, and an even, smooth perovskite surface could promote this interface to integrate entirely. The poor contact could seriously suppress the device performance, especially the short-circuit photocurrent density (J_{SC}) and the fill factor (FF).[28–30] After optimization, a champion device with an open-circuit voltage (V_{OC}) of 921 mV, a J_{SC} of 17.94 mA·cm^{-2}, an FF of 60.6%, and a PCE of 10.02% was achieved.

2. Experiments

2.1. Materials

All the chemicals were used as received. FTO glass (15 Ω/□), lead iodide (99.9%), CH_3NH_3I (99.5%), and TiO_2 paste (Dyesol 18NR-T) were purchased from Ying Kou You Xuan Trade Co., Ltd. TiO_2 compact layer solution (NJU-DL) was purchased from Kunshan Sunlaite New Energy Co., Ltd. Ethanol (99.7%), isopropanol (99.7%), toluene (99.5%), and diethyl ether (99.5%) were purchased from Sinopharm Chemical Reagent Co., Ltd. N,N-dimethylformamide (DMF, 99.8%), dimethyl sulfoxide (DMSO, 99.8%), and chlorobenzene (99.5%) were purchased from Aladdin Industrial Corporation.

2.2. Device fabrication

The device structure in this work is shown in Fig. 1. The FTO substrates were cleaned sequentially in acetone, ethanol, and deionized water by ultrasonication for 10 min respectively. After being dried in a drying oven, they were exposed to UV-ozone radiation for 15 min. A compact TiO_2 layer was deposited onto the substrate by spin-coating the TiO_2 solution (NJU-DL) at 4500 rpm for 30 s and then sintered at 500 °C for 30 min. Next, a mesoporous TiO_2 layer was deposited onto the substrate by spin-coating the TiO_2 paste (Dyesol 18NR-T) which was diluted in ethanol (1:6, weight ratio) at 5000 rpm for 30 s and then sintered at 500 °C for 30 min. The perovskite layer was prepared by an antisolvent extraction strategy based on the two-step sequential method. A 1.2 M solution of PbI_2 in a mixed solvent of DMF and DMSO (DMSO: $PbI_2 = 1:1$, molar ratio) was spin-coated onto the mesoporous TiO_2 layer at 3000 rpm for 30 s. The PbI_2 solution was filtered through a PTFE filter (0.13 μm) and kept at 70 °C before usage. Samples without antisolvent extraction treatment were then annealed on a hot plate at 70 °C for 30 min. Samples with treatment were prepared as follows: about 400 μL antisolvent (CB, TL, or DE) was dripped onto the as-deposited PbI_2 film smoothly and quickly for different loading time: 5 s (operating time), 15 s, and 25 s. After being spun again at 3000 rpm for 30 s, the films were also annealed at 70 °C for 30 min. After that, the PbI_2 films were immersed in a 15 mg/mL CH_3NH_3I (MAI)/isopropanol (IPA) solution for different lengths of time: 1 min, 5 min, 10 min, and 30 min for samples with antisolvent extraction treatment and 20 min, 30 min, 40 min, and 60 min for samples without the treatment. Then the films were washed in an IPA solvent to remove redundant MAI and spun to dry at 3000 rpm for 15 s. Finally, the perovskite films were annealed at 100 °C for 20 min. A commercial carbon paste was directly painted onto the surface of the perovskite layers and then annealed at 120 °C for 20 min to form the carbon electrode.

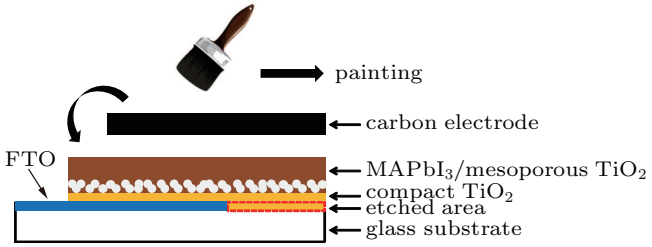


Fig. 1. (color online) The device structure of PC-based perovskite solar cells in this work.

2.3. Characterization

The x-ray diffraction (XRD) patterns were measured by a RU-200B/D/MAX-RB RU-200B rotation anode high power x-ray diffractometer. The surface morphologies of the perovskite films and the cross-sectional morphologies of the whole devices were obtained from a Hitachi S-4800 field emission scanning electron microscope (SEM). The atomic force microscope (AFM) images were obtained by a CSPM4000 scanning probe microscope. The device photovoltaic parameters including the current density–voltage curves were measured with a Keithley 2400 source meter under AM 1.5G one-sun illumination provided by a solar simulator (Oriel Sol 3A class AAA).

3. Results and discussion

Figure 2 shows the detailed preparation procedures of the perovskite layers in our experiments. The entire experiment can be divided into two stages. In the first stage, the predeposited PbI_2 films were divided into three groups and treated with CB, TL, and DE, respectively. Drops of antisolvents were directly loaded onto the PbI_2 substrates with different waiting time (5 s, 15 s, and 25 s). The extraction time was set up according to the previous report and adjusted for the experimental conditions in this work.[20] Then the PbI_2 films with antisolvent extraction treatment were immersed in an MAI/IPA solution for 30 min. In the first stage, the optimal extraction time was determined for the next stage. In the second stage, the antisolvent treated PbI_2 films with optimal extraction time and the PbI_2 films without treatment were immersed

in the MAI/IPA solution for different lengths of time. The soaking time for films with antisolvent treatment was 1 min, 5 min, 10 min, and 30 min; and for films without treatment was 20 min, 30 min, 40 min, and 60 min.[19,31] In this stage, the optimal soaking time was determined. The photovoltaic parameters of the PSCs in the first stage are listed in Table 1. Samples were recorded as **-5, **-15, and **-25 PSCs (** represents that antisolvents were used, and numbers indicate the extraction time). Both the CB and TL treated PSCs showed that the PCE increases with longer extraction time. The DE-treated samples did not show this trend mostly because of its fast evaporation rate. An overlong extraction time ($\geq$ 15 s) for DE would lead to random and irregular damage to the morphologies of the PbI_2 films. Similar phenomena were observed in CB and TL treated samples with extraction time $\geq$ 40 s. Thus the optimal extraction time was determined, which was 25 s for CB and TL and 5 s for DE.

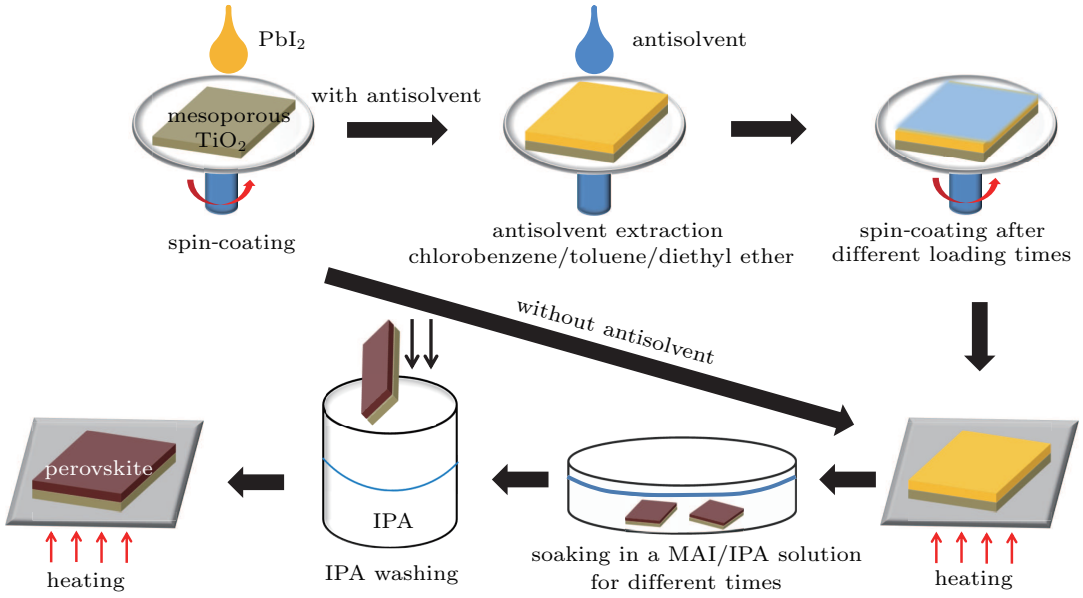


Fig. 2. (color online) Schematic of the preparation procedures of perovskite layers with or without antisolvent extraction treatment on PbI_2 films.

Table 1. Photovoltaic parameters of PSCs treated with different antisolvents and extraction time. The soaking time was set at 30 min. All the values were averaged from at least 5 devices.

Experimental groups	Extraction time/s	V_{OC}/mV	J_{SC}/mA·cm^{-2}	*FF*/%	PCE/%
CB	5	884	11.25	48.0	4.77
	15	928	9.10	57.7	4.87
	25	909	10.28	60.0	5.61
TL	5	948	4.71	43.7	1.95
	15	927	9.79	51.0	4.63
	25	897	10.75	55.0	5.30
DE	5	936	10.05	50.4	4.74
	15	937	6.87	36.3	2.34
	25	918	9.30	43.2	3.69

In the second stage, the soaking time of the antisolvent treated samples with the optimal extraction time was studied. The optimal soaking time for samples without the treatment was also included. Figure 3 shows the XRD patterns of the perovskite films prepared by different antisolvent extraction treatments or no treatment. The diffraction peaks at around 14.1°, 24.4°, 28.4°, 31.8°, and 37.6° can be assigned to the (110), (202), (220), (310), and (312) planes of the tetragonal perovskite structure.[32,33] The diffraction peak at around 12.6° can be assigned to the (001) plane of the hexagonal PbI_2.[20] All the perovskite films prepared by antisolvent extraction treatments showed PbI_2 residual when the soaking time was less than 10 min. In Fig. 3(c), the TL treated perovskite films showed an obvious diffraction peak at 12.6° even when the soaking time was prolonged to 30 min, which indicates that the transformation of PbI_2 to perovskite was quite slow and considerable amount of PbI_2 was left. It is believed that when MAI inserts into the PbI_2 crystal lattice, the grain volume would expand and result in a compact perovskite layer capping on the surface of the PbI_2 film which blocks the further diffusion and insertion of MAI.[34] This would lead to an incomplete transformation of PbI_2 to perovskite and degrade the device performance since the residual PbI_2 would slow down the electron separation and transportation.[35] By

comparing the diffraction peaks at 12.6° from W/O-30 PSCs in Fig. 3(a) and CB-30 PSCs in Fig. 3(b), the CB samples were found to show a faster transformation of PbI_2 to perovskite. This is because the CB extraction treatment can change the PbI_2 film to a porous status, which accelerates the transformation process.[36] In Fig. 3(d), the DE-treated samples showed much better XRD spectra when the extraction time was prolonged to 30 min, which indicates that perovskite films with no PbI_2 residual and high crystallinity were obtained. All experimental groups showed stronger perovskite diffraction peaks with longer soaking time, especially the (110) and (220) planes, demonstrating that higher crystallinity films were obtained. The photovoltaic parameters of the PSCs in the soaking time experiments are summarized in Table 2. The *J*–*V* curves of the best performance PSCs from each experimental group are shown in Fig. 4.

Table 2. Photovoltaic parameters of PSCs in the soaking time experiments. All the values were averaged from at least 5 devices.

Experimental groups	Soaking time/min	V_{OC}/mV	J_{SC}/mA·cm^{-2}	*FF*/%	PCE/%
W/O	20	923	17.28	50.5	8.05
	30	944	15.90	55.4	8.32
	40	925	16.88	60.3	9.42
	60	890	16.27	55.1	7.98
CB-25	1	962	11.29	40.8	4.43
	5	952	10.04	47.4	4.53
	10	943	10.86	50.9	5.21
	30	909	10.28	60.0	5.61
TL-25	1	968	4.77	44.3	2.05
	5	983	3.85	40.3	1.53
	10	963	9.30	43.0	3.85
	30	897	10.75	55.0	5.30
DE-5	1	969	5.80	34.5	1.94
	5	959	9.21	39.9	3.52
	10	948	8.94	43.7	3.70
	30	936	10.05	50.4	4.74

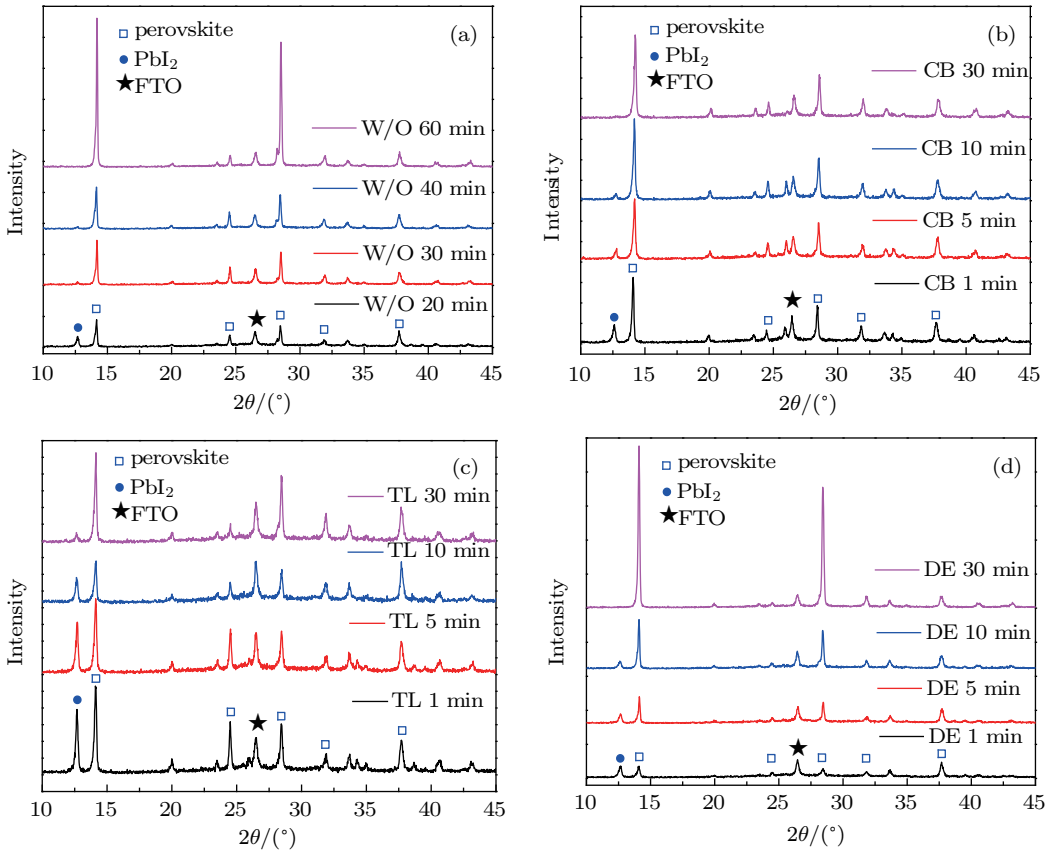


Fig. 3. (color online) XRD patterns of perovskite films prepared by (a) non-antisolvent extraction treatment, (b) CB extraction treatment with an extraction time of 25 s, (c) TL extraction treatment with an extraction time of 25 s, and (d) DE extraction treatment with an extraction time of 5 s.

We found the optimal soaking time was 40 min for W/O samples and 30 min for samples treated with CB, TL, and DE. The best samples in different groups were recorded as W/O-40 PSCs, CB-30 PSCs, TL-30 PSCs, and DE-30 PSCs. The W/O-40 PSCs showed the best performance with a V_{OC} of 925 mV, a J_{SC} of 16.88 mA·cm^{-2}, an FF of 60.3%, and a PCE of 9.42%. The corresponding XRD spectra indicated that almost no redundant PbI_2 remained. However, an overlong soaking time (60 min) was not suitable for W/O samples despite the fact that the perovskite diffraction peaks became stronger (see Table 2). With the ion migration process during film growth, a dissolution-recrystallization process would occur in the perovskite layer and large sparsely distributed perovskite crystals would form on the surface.[19] This demonstrated that an overlong soaking time was improper for high-quality perovskite films and thus led to lower PCE.

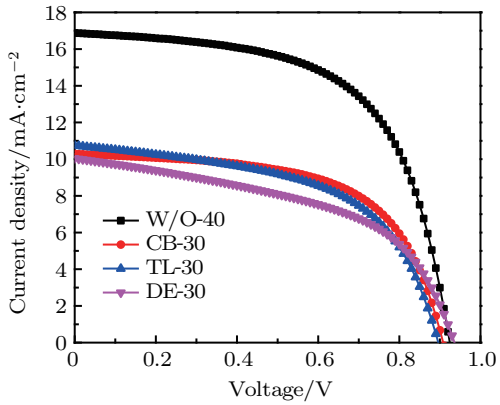


Fig. 4. (color online) J–V curves of the best performance PSCs from each experimental group in the soaking time experiments.

The surface SEM images of the perovskite films from W/O-40, CB-30, TL-30, and DE-30 PSCs are shown in Fig. 5. Except for the DE-30 PSCs, the surface morphologies of these perovskite films were similar with a full perovskite coverage and very few pinholes. Their grains were uniform with sizes of about 200–300 nm. By contrast, the DE-30 PSCs showed inferior perovskite surface morphologies. A poor perovskite coverage and a considerable quantity of pinholes could be observed in Fig. 5(d). The crystal sizes were relatively smaller ($\leq$ 200 nm) and thus brought more grain boundaries. These pinholes and grain boundaries caused more charge recombination and bigger series resistance due to the large density of charge traps.[37] Thus the photocurrent density and fill factor were reduced severely. AFM was performed to further explore the topographies of these perovskite films. As shown in Fig. 6, the average roughnesses of the perovskite films were 32.5 nm for W/O-40 PSCs, 66.3 nm for CB-30 PSCs, 66.7 nm for TL-30 PSCs, and 68.6 nm for DE-30 PSCs. All the perovskite films prepared by antisolvent extraction treatment were rougher than the films without treatment. A reasonable explanation is that when antisolvents were introduced to PbI_2 films, the organic solvent in the precursor solution was removed too fast for the PbI_2 crystal particles to crystallize slowly and uniformly. Large grain particles or even bulks gathered on the film surface and brought undesired surface fluctuations. Thus the perovskite films prepared subsequently showed uneven surfaces. Lots of research has demonstrated that many kinds of solvent treatment methods could turn PbI_2 films into a porous status as the CB extraction treatment did.[36,38,39] Though a porous structure made the transformation from PbI_2 to perovskite faster and completed, increased surface roughness was also observed from the perovskite films.[34]

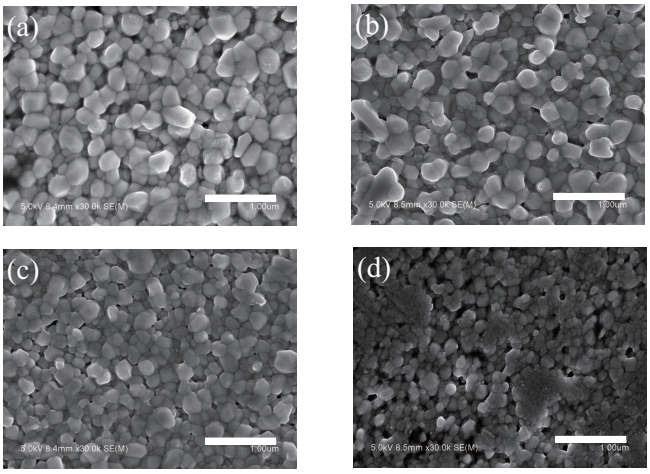


Fig. 5. Surface SEM images of the perovskite films from (a) W/O-40, (b) CB-30, (c) TL-30, and (d) DE-30 PSCs. The scale bars represent 1 μm.

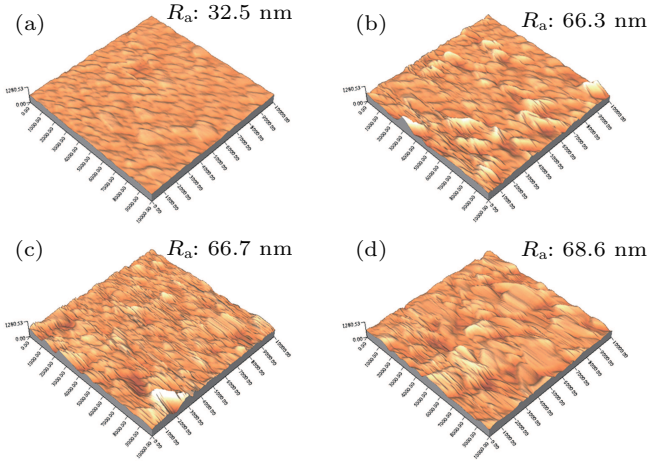


Fig. 6. (color online) AFM images of the perovskite films from (a) W/O-40, (b) CB-30, (c) TL-30, and (d) DE-30 PSCs.

Figure 7 shows the cross-sectional SEM images of the best performance PSCs in these four experimental groups. Combined with the AFM results, it could be inferred that a rough surface aggravated the poor contact between the perovskite layer and carbon electrode. The surface fluctuations in the perovskite films may lead to an empty hole in the perovskite/carbon electrode interface because of a bump on the

perovskite surface, as circled in Fig. 7(b); an uncovered area because of a hollow, as in Fig. 7(c); or even a capping layer levitating above the film surface, as in Fig. 7(d). Due to an uneven perovskite surface, every situation is possible at the contact interface, resulting in a poor contact status. Moreover, the carbon paste was viscous and abundant of organic solvents (such as epoxy) and a direct painting method was utilized to prepare the carbon electrode. Unlike HTM-based PSCs wherein the hole-transport-layers or metal electrodes are deposited onto the perovskite surface in a molecular or atomic scale by specialized techniques (e.g., thermal evaporation method), the painted carbon electrode may be deposited in a micron scale. The inherent nature of carbon paste and the painting technique used in PC-based PSCs made it hard to fulfill the complete contact between the perovskite layer and carbon electrode. Figure 7(a) shows a relatively better contact status of W/O-40 PSCs. According to the topographies from the AFM images and the contact problems from the cross-sectional SEM images, a simple diagram is displayed in Fig. 7(e) to illustrate the contact status of the perovskite/carbon electrode interface. The rightmost circled area shows a more compact contact owing to a flat perovskite surface compared with the other three cases.

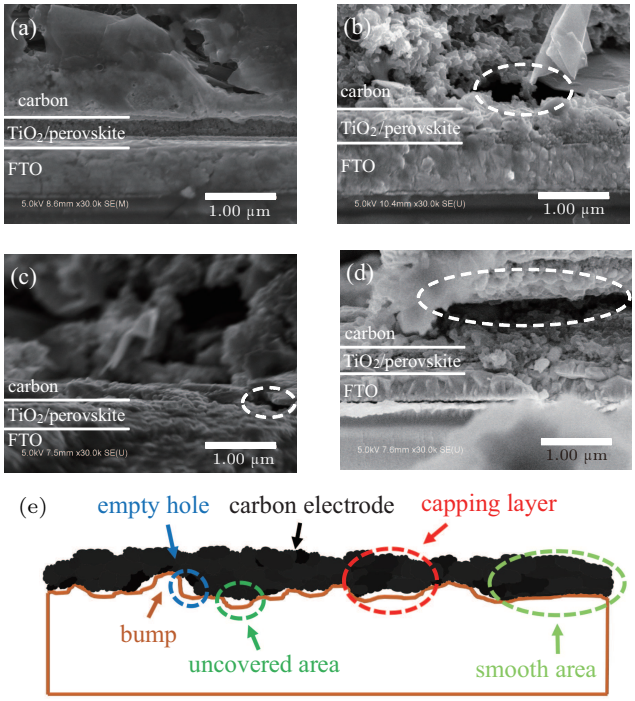


Fig. 7. (color online) Cross-sectional SEM images of (a) W/O-40, (b) CB-30, (c) TL-30, and (d) DE-30 PSCs. The scale bars represent 1 μm. (e) A simulated diagram of the perovskite/carbon electrode interface.

Table 3 summarizes the influencing factors and performance of W/O-40, CB-30, TL-30, and DE-30 PSCs. The CB-30 PSCs were used as the reference. With a little PbI_2 residual, the PCEs of the TL-30 PSCs decreased by 6% compared to that of the reference cells. The DE-30 PSCs lost 16% in PCEs as a result of poor surface morphology. The compact perovskite/carbon electrode contact of W/O-40 PSCs helped to enhance the PCEs by 68%. Clearly, the contact status between the perovskite layer and the carbon electrode dominated the device performance in PC-based PSCs. A flat and smooth perovskite surface would also greatly assist PCEs improvement. No PbI_2 residual and good surface morphologies could help to improve the device performance but their influence was not as significant as that of the contact status. W/O-40 PSCs showed the best performance in all the experiments. After optimization, the highest PCE up to 10.02% was achieved. The *J*–*V* curve and photovoltaic parameters are shown in Fig. 8.

Table 3. Comparison between influencing factors and performance of PSCs in the soaking time experiments.

Influencing factors	W/O-40	CB-30	TL-30	DE-30
PbI_2 residual	none	none	a little	none
Surface morphology	good	good	good	poor
Surface roughness/nm	32.5	66.3	66.7	68.6
Perovskite/carbon electrode contact	compact	poor	poor	poor
PCE/%	9.42	5.61	5.30	4.74

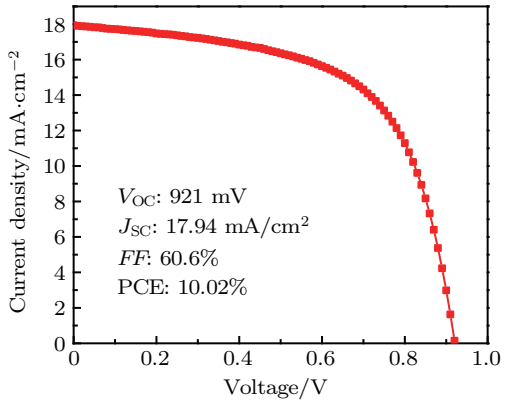


Fig. 8. (color online) The *J*–*V* curve and photovoltaic parameters of the champion PSC from W/O-40 PSCs.

4. Conclusion

By comparing the device performance of PC-based PSCs prepared with or without the antisolvent extraction treatment, we demonstrated that the dominating factor of PC-based PSCs performance is the contact status of the perovskite/carbon electrode interface. An even perovskite surface can be a great help to improve the contact status. The effects of the other two factors (PbI_2 residual and the surface morphology) were limited in the case of a poor contact, even though they are crucial in HTM-based PSCs. CB-30 PSCs exhibited the highest PCEs among all the antisolvent-treated samples, however, their PCEs improvement was limited compared with the PSCs

treated with TL and DE. The poor contact between the perovskite layer and carbon electrode resulting from a rough perovskite surface seriously influenced their PCEs. To conclude, a good perovskite/carbon electrode contact should be the prime requisite in high-performance PC-based PSCs.

References

[1] Kojima A, Teshima K, Shirai Y and Miyasaka T 2009 *J. Am. Chem. Soc.* **131** 6050
[2] Lee M M, Teuscher J, Miyasaka T, Murakami T N and Snaith H J 2012 *Science* **338** 643
[3] Bi D, Xu B, Gao P, Sun L, Grätzel M and Hagfeldta A 2016 *Nano Energy* **23** 138
[4] Chai L and Zhong M 2016 *Acta Phys. Sin.* **65** 237902 (in Chinese)
[5] Im J H, Kim H S and Park N G 2014 *APL Mater.* **2** 081510
[6] Li X, Bi D, Yi C, Décoppet J D, Luo J, Zakeerudin S M, Hagfeldt A and Grätzel M 2016 *Science* **353** 58
[7] Jeon N J, Noh J H, Kim Y C, Yang W S, Ryu S and Seok S I 2014 *Nat. Mater.* **13** 897
[8] Xia C, Song W D, Zhang C Z, Yuan S Y, Hu W X, Qin P, Wang R P, Zhao L L, Wang X F, He M and Li S T 2017 *Chin. Phys. B* **26** 018401
[9] Hsiao S Y, Lin H L, Lee W H, Tsai W L, Chiang K M, Liao W Y, Ren-Wu C Z, Chen C Y and Lin H W 2016 *Adv. Mater.* **28** 7013
[10] Jia E D, Lou X, Zhou C L, Hao W C and Wang W J 2017 *Chin. Phys. B* **26** 068803
[11] Liu Y, Xu Z, Zhao S L, Qiao B, Li Y, Qin Z L and Zhu Y Q 2017 *Acta Phys. Sin.* **66** 118801 (in Chinese)
[12] Chen C W, Kang H W, Hsiao S Y, Yang P F, Chiang K M and Lin H W 2014 *Adv. Mater.* **26** 6647
[13] Liu P, Yang B C, Liu G, Wu R S, Zhang C J, Wan F, Li S G, Yang J L, Gao Y L and Zhou C H 2017 *Chin. Phys. B* **26** 058401
[14] Li J F, Zhao C, Zhang H, Tong J F, Zhang P, Yang C Y, Xia Y J and Fan D W 2016 *Chin. Phys. B* **25** 028402
[15] Stranks S D, Eperon G E, Grancini G, Menelaou C, Alcocer M J, Leijtens T, Herz L M, Petrozza A and Snaith H J 2013 *Science* **342** 341
[16] Etgar L, Gao P, Xue Z, Peng Q, Chandiran A K, Liu B, Nazeeruddin M K and Grätzel M 2012 *J. Am. Chem. Soc.* **134** 17396
[17] Chen H, Wei Z, Zheng X and Yang S 2015 *Nano Energy* **15** 216
[18] Wei H, Xiao J, Yang Y, Lv S, Shi J, Xu X, Dong J, Luo Y, Li D and Meng Q 2015 *Carbon* **93** 861
[19] Chen H, Wei Z, He H, Zheng X, Wong K S and Yang S 2016 *Adv. Energy Mater.* **6** 1502087
[20] Zhang J, Zhai G, Gao W, Zhang C, Shao Z, Mei F, Zhang J, Yang Y, Liu X and Xu B 2017 *J. Mater. Chem. A* **5** 4190
[21] Chen H and Yang S 2017 *Adv. Mater.* **29** 1603994
[22] Zhang C X, Luo Y D, Chen X H, Chen Y W, Sun Z and Huang S M 2016 *Nano-Micro Lett.* **8** 347
[23] Sakai N, Pathak S, Chen H W, Haghighirad A A, Stranks S D, Miyasaka T and Snaith H J 2016 *J. Mater. Chem. A* **4** 4464
[24] Ryu S, Seo J W, Shin S S, Kim Y C, Jeon N J and Noh J H 2015 *J. Mater. Chem. A* **3** 3271
[25] Yu Y, Yang S, Lei L, Cao Q, Shao J, Zhang S and Liu Y 2017 *ACS Appl. Mater. Interfaces* **9** 3667
[26] Luo P, Liu Z, Xia W, Yuan C, Cheng J and Lu Y 2015 *ACS Appl. Mater. Interfaces* **7** 2708
[27] Tai Q, You P, Sang H, Liu Z, Hu C, Chan H L, Helen L W and Yan F 2016 *Nat. Commun.* **7** 11105
[28] Zhang F, Yang X, Wang H, Cheng M, Zhao J and Sun L 2014 *ACS Appl. Mater. Interfaces* **6** 16140
[29] Zhou H, Shi Y, Dong Q, Zhang H, Xing Y, Wang K, Du Y and Ma T 2014 *J. Phys. Chem. Lett.* **5** 3241
[30] Chen H, Wei Z, Zheng X and Yang S 2015 *Nano Energy* **15** 216
[31] Fu Y, Meng F, Rowley M B, Thompson B J, Shearer M J, Ma D, Hamers R J, Wright J C and Jin S 2015 *J. Am. Chem. Soc.* **137** 5810
[32] Liao G, Liu Z, Shi T, Tang Z and Sun B 2016 *Nanoscale* **8** 7017
[33] Luo Q, Ma H, Zhang Y, Yin X, Yao Z, Wang N, Li J, Fan S, Jiang K and Lin H 2016 *J. Mater. Chem. A* **4** 5569
[34] Zhang T, Yang M, Zhao Y and Zhu K 2015 *Nano Lett.* **15** 3959
[35] Chiang C H, Nazeeruddin M K, Grätzel M and Wu C G 2017 *Energy Environ. Sci.* **10** 808
[36] Li M, Yan X, Kang Z, Liao X, Li Y, Zheng X, Lin P, Meng J and Zhang Y 2017 *ACS Appl. Mater. Interfaces* **9** 7224
[37] Zhang Y, Wang Y, Sun Z, Li F, Tao R, Jin Z and Xu L 2017 *Chem. Commun.* **53** 2290
[38] El-Henawey M I, Gebhardt R S, El-Tonsy M M and Chaudhary S 2016 *J. Mater. Chem. A* **4** 1947
[39] Wang Y, Li S, Zhang P, Liu D, Gu X, Sarvari H, Ye Z, Wu J, Wang Z and Chen Z D 2016 *Nanoscale* **8** 19654